Spin reorientation transition and magnetic domain structure of Co ultrathin films grown on a faceted Au(455) surface

J. H. Gao,[1] Y. Girard,[1,*] V. Repain,[1] A. Tejeda,[1] R. Belkhou,[2] N. Rougemaille,[3] C. Chacon,[1] G. Rodary,[1] and S. Rousset[1]
[1]*Laboratoire Matériaux et Phénomènes Quantiques, CNRS—Université Paris 7, 10 rue Alice Domon et Léonie Duquet, 75205 Paris Cedex 13, France*
[2]*Synchrotron SOLEIL, L'Orme des Merisiers, Saint-Aubin, Boîte Postale 48, 91192 Gif-sur-Yvette Cedex, France*
[3]*Institut Neél, CNRS & Université Joseph Fourier, Boîte Postale 166, F-38042 Grenoble Cedex 9, France*
(Received 27 July 2007; revised manuscript received 3 March 2008; published 16 April 2008)

The spin reorientation transition (SRT) and magnetic domain structure of Co ultrathin films on faceted Au(455) surfaces have been investigated as a function of thickness by using magneto-optic Kerr effect and x-ray photoemission electron microscopy in combination with x-ray magnetic circular dichroism. The magnetization easy axis of the Co films is found to rotate from an out-of-plane to an in-plane orientation perpendicular to the atomic steps of the substrate due to the dominant contribution of the step-induced magnetic anisotropy. Moreover, magnetic stripe domains are observed to replicate the underlying periodic facets of the Au surface. Depending on the facet, the SRT occurs at a well-defined critical thickness and proceeds via a different mechanism: a state of uniform canted magnetization is formed for (233) facets, while the SRT involves continuous magnetization rotation followed by the nucleation of small in-plane magnetic domains for (677) facets.

DOI: 10.1103/PhysRevB.77.134429 PACS number(s): 75.30.Gw, 68.37.Xy, 75.70.Kw, 75.70.Ak

I. INTRODUCTION

Low-dimensional magnetism, which combines basic fundamental research and potential technological applications in information processing and storage devices, has grown to become an active and promising field of investigation in condensed matter physics.[1,2] The drastic development of research on magnetic nanostructures has greatly benefited from the progresses of synthesis techniques.[3] Among them, advanced nanolithography offers extraordinary possibilities to fabricate well-defined homogeneous nanostructures, with controlled size and shape. However, they are difficult to fabricate on a large scale, mainly because of high cost and time consumption. An alternative approach to overcome these inconveniences is self-organization. In particular, atomic beam epitaxy on periodic patterns (such as strain relief patterns, for example) on single crystal surfaces has been shown to provide very good templates for nanostructures.[4–7]

For monolayer-thick magnetic films, many interesting effects have been observed, among which two aspects have attracted particular attention: magnetic domain structure and spin reorientation transition (SRT) phenomena.[8–10] The equilibrium magnetic domain structure is determined by the competition between exchange, dipolar, and anisotropy energies, while the effective magnetic anisotropy constant governs the direction of magnetization. Because of the broken symmetry in low-dimensional systems, surface and interface magnetic anisotropies often play an important role in stabilizing an out-of-plane alignment of the magnetization in ultrathin magnetic structures. With increasing material thickness, the influence of the interface decreases, and dipolar interaction gains strength. Then, demagnetization energy usually forces the magnetization to lie within the film plane. More generally, any variation in the magnetic anisotropies, for example, due to a modification of thickness[11,12] or temperature,[13,14] could result in a change of the magnetization direction, i.e., SRT.

Experiments on SRT in ultrathin films have revealed that magnetic microstructures can determine the magnetic behavior of the system to a large extent. Consequently, the study of magnetic domain structure has attracted much interest in understanding SRT phenomena and magnetic long-range order in magnetic ultrathin films. Theoretically, it is found that the magnetic stripe domain phase has a lower energy than the single domain phase. In addition, it is predicted that the stripe domain width should rapidly shrink toward a minimum value as the total effective magnetic anisotropy approaches zero. Experimentally, the existence of the magnetic stripe phase at the SRT was verified in Fe/Cu(100) (Refs. 15 and 16) and coupled magnetic sandwiches.[17–19] Recent studies have also proved that a new metastable magnetic phase—a bubble domain phase[20]—could be stabilized within a narrow SRT region. The discovery of this magnetic domain phase has stimulated many research activities to investigate domain dynamics, phase transitions, and ground-state spin structures. Both the spin reorientation transition and the magnetic microstructure of monolayer thick-Co films grown on Au(111) have been investigated.[21–23] In this system, Co films exhibit large out-of-plane magnetized domains with a typical size of several microns. In the vicinity of the SRT, the domain size decays down to about 200–300 nm, with in-plane and out-of-plane domains coexisting in a narrow thickness range.

Here, we briefly recall the geometry of the faceted Au(455) surface. More detailed information can be found elsewhere.[24–26] Au(455) surface is a (111) vicinal surface misoriented toward the $[\bar{2}11]$ direction, which exhibits hill-and-valley morphology with a period of facets of a few hundred nanometers. Typical STM images of the Au(455) surface are shown in Fig. 1, which reveal that the Au(455) surface is made up of two different vicinal surfaces—Au(677) and Au(233) facets, with the width of (677) facet slightly larger than one of (233) facet. The corresponding

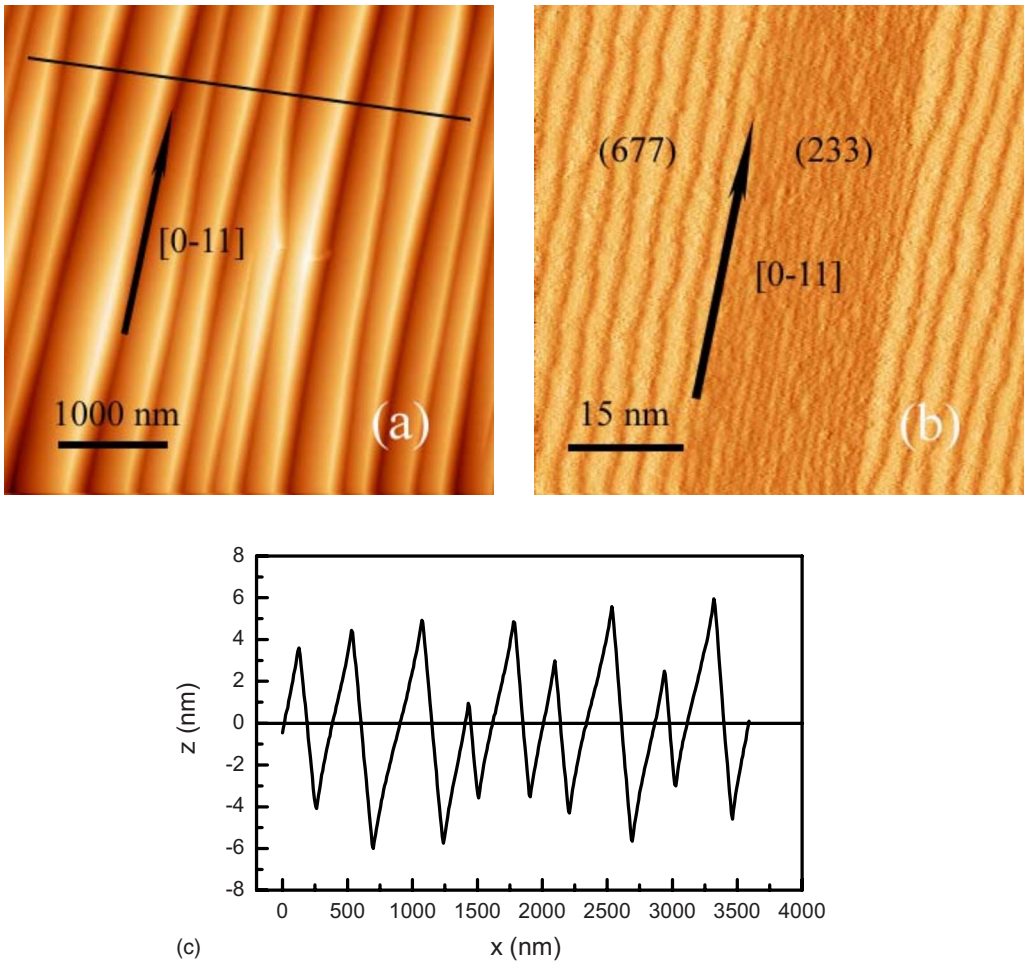

FIG. 1. (Color online) Morphology of the Au(455) surface. (a) 4000×4000 nm^2 STM image of the Au(455) surface. (b) 60×60 nm^2 STM image of the faceted edge area on Au(455) surface. (c) Profile distribution of the Au(455) surface in (a).

vicinal angles with respect to the [111] direction are $\theta_1=+3°$ and $\theta_2=-4°$ along the $[\bar{2}11]$ direction for (677) and (233) facets, respectively, with the steps being parallel to the $[0\bar{1}1]$ direction. Previous magnetic investigations were performed on Au/Co/Au(455) (Ref. 27) by magneto-optical Kerr effect (MOKE) measurements and magneto-optical Kerr microscopy. For Au (7.0 ML)/Co (4.0 ML)/Au(455) films, magnetic hysteresis loops describe the average of the magnetization on each facet: one lying in plane and the other staying out of plane. The step density of the vicinal surface has a dramatic effect on the magnetic anisotropy, the facet with a high step density displaying in-plane anisotropy and the other facet exhibiting perpendicular anisotropy. Calculations[24] also predicted that Au(455) vicinal surfaces can induce a periodic anisotropy modulation due to the magnetoelastic effects on facet edges. From Kerr microscopy, it is observed that the domain wall propagation is highly anisotropic, with an easy propagation direction parallel to the step direction.

In this paper, we focus on the magnetic domain structure of Co/Au(455) films during the out-of-plane to the in-plane SRT. Our experimental results show that the SRT occurs with a rotation of the magnetization easy axes from out of plane to in plane, with an in-plane preferred orientation perpendicular to the steps. X-ray photoemission electron microscopy (X-PEEM) experiments in combination with x-ray magnetic circular dichroism (XMCD) clearly show that magnetic domains replicate the hill-and-valley shape of the Au substrate. We also evidence that with increasing Co film thickness, two different kinds of SRT processes take place within the two facets: continuous canting of magnetization in (233) facets and formation of small in-plane magnetized domains in (677) facets.

II. EXPERIMENTAL DETAILS

Experiments were performed in an ultrahigh vacuum chamber with a base pressure below 1.0×10^{-10} mbar. Au(455) surfaces were prepared by using a standard method: Ar^+ sputtering at 900 eV kinetic energy followed by a short annealing at 800 K. Co ultrathin films were deposited onto the Au(455) surface at room temperature with a vacuum pressure below 5.0×10^{-10} mbar. Cobalt films were evaporated with a typical deposition rate of 0.1 ML/min. Magnetic hysteresis loops were recorded *in situ* during the film growth at room temperature by using polar and longitudinal MOKE configurations with maximum applied magnetic fields of 800 and 2500 Oe, respectively.

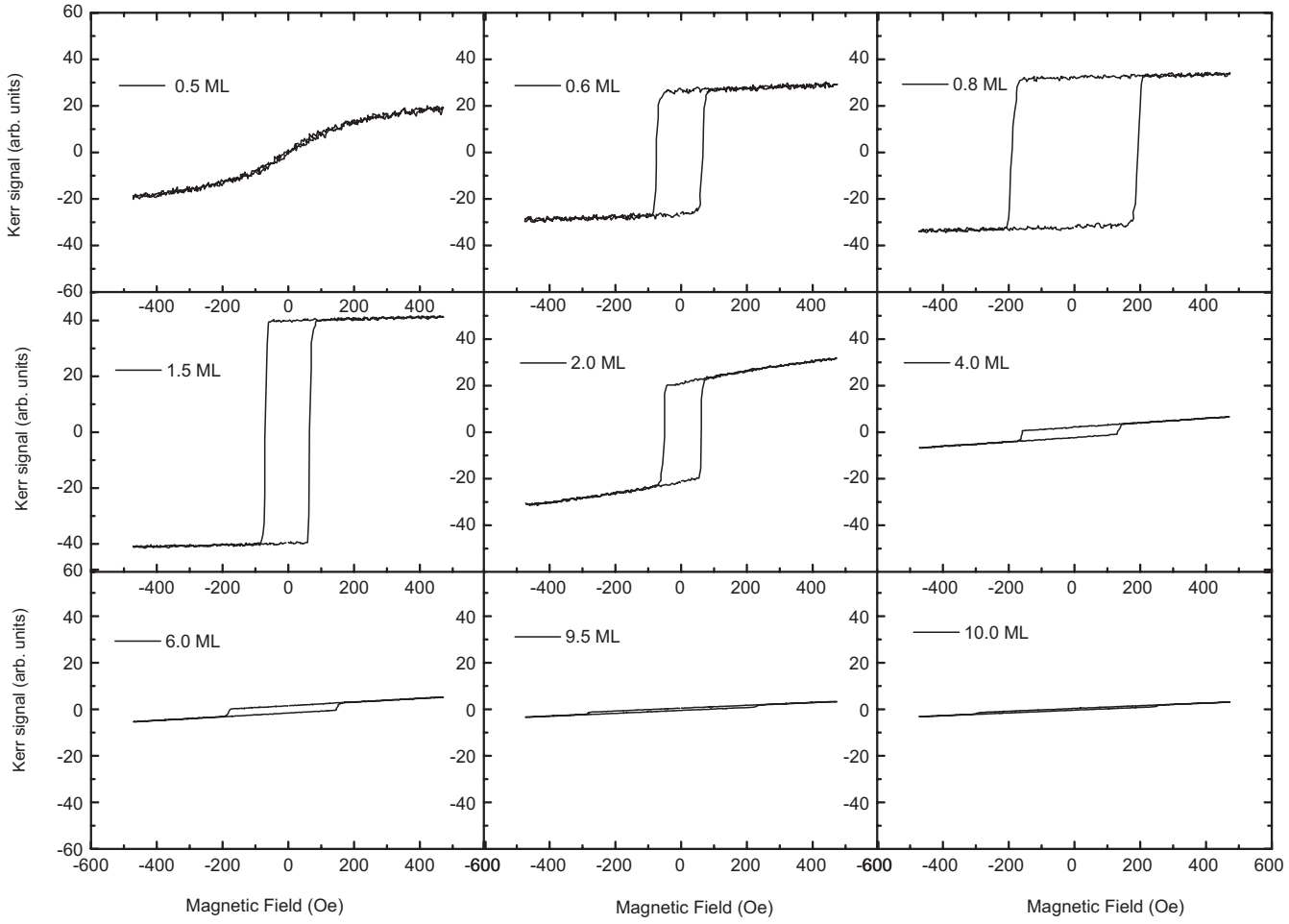

FIG. 2. Typical MOKE hysteresis loops that are obtained in the polar configuration from Co films grown on Au(455) surface for different film thicknesses.

X-PEEM measurements were carried out at the Elettra synchrotron facility (Nanospectroscopy beamline) in Trieste (Italy). Co was evaporated *in situ* inside the microscope chamber and the deposition rate was calibrated prior to the experiments by observing the growth of Co on a W(110) sample. Magnetic images of the Co films were obtained at the Co L_3 edge, with an incident x-ray beam at 74° with respect to the surface normal direction. To obtain a good signal to noise ratio in these images, sequences of images were taken for each helicity of the circularly polarized light, which is subtracted and normalized to the sum. A local XMCD signal was deduced from the two X-PEEM images excited by right (I_+) and left (I_-) circularly polarized lights by using the expression $I_{asy}=(I_- - I_+)/(I_- + I_+)$. I_{asy} is proportional to cos φ, where φ is the angle between incident polarized x rays and local magnetization. In the images shown here, the typical resolution is 30 nm and a field of view is 5.0 μm.

III. RESULTS AND DISCUSSION

A. Magneto-optical Kerr effect measurements

Magnetic hysteresis loops of Co ultrathin films on faceted Au(455) surfaces are investigated by *in situ* MOKE as a function of Co coverage. Figure 2 shows the typical hysteresis loops that are obtained at room temperature for different film coverages. There, the polar configuration is used to measure the out-of-plane component of the magnetization. For films thinner than 0.5 ML, no remanence magnetization signal is obtained, and Co nanostructures exhibit a superparamagnetic behavior since the critical temperature for ferromagnetic order is below room temperature.[28] For coverages thicker than 0.6 ML, Co films exhibit square hysteresis loops with full remanence, indicating that the easy axis of magnetization (EAM) is perpendicular to the film plane. The change in shape of the hysteresis loops between 0.5 and 0.6 ML corresponds to the transition from superparamagnetism to ferromagnetism. This perpendicular magnetic anisotropy is commonly ascribed to the dominant role of the interface anisotropy between the substrate and the film.[28] When the film thickness further increases (up to around 2.0 ML), Co films exhibit canted hysteresis loops with a small remanence, showing that the SRT from an out-of-plane to an in-plane orientation has occurred. The detailed SRT behavior will be analyzed in Sec. III B. For films thicker than 10.0 ML, linear hysteresis loops are found, indicating that the magnetization completely lies in the film plane. Figure 3 shows the remanence squareness (M_R/M_S) that is obtained from the hysteresis loops as a function of the film thickness in (a) the polar

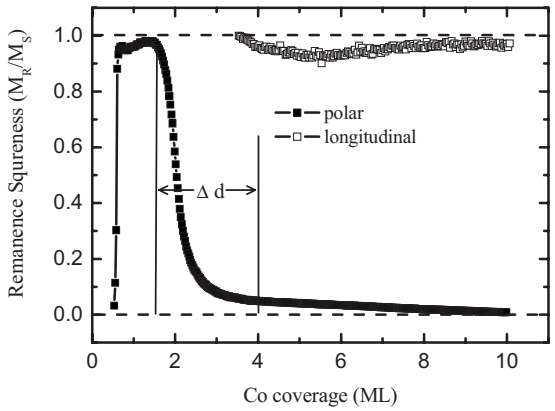

FIG. 3. Remanence squareness that is obtained from hysteresis loops in the polar (solid squares) and longitudinal (open squares) (with magnetic field perpendicular to the steps) MOKE configurations as a function of the film thickness.

and (b) longitudinal (with the magnetic field applied in plane, perpendicular to the steps) MOKE configurations. The value of the remanence squareness around 1.0 corresponds to the preferred magnetization direction. From the variation in remanence squareness in the polar configuration, we deduce that the SRT takes place for a thickness ranging between 2.0 and 4.0 ML (note that for a 4.0 ML thick film, the remanence squareness in the polar configuration is still of 4.8%, i.e., an out-of-plane component of the magnetization still exists).

For Co/Au(111) films, isotropic in-plane magnetic domain shapes were reported that show no preferential[21] in-plane magnetization axis. However, it is known that atomic steps of vicinal surface induce uniaxial magnetic anisotropy since the directions parallel and perpendicular to the steps are not equivalent (symmetry breaking). Then, for stepped surfaces, there should exist an easy magnetization direction within the film plane. We have investigated this effect on Au(455). MOKE measurements in the longitudinal configuration were performed as a function of Co coverage with the magnetic field applied parallel and perpendicular to the steps (see Fig. 4). When the magnetic field is perpendicular to steps (a)–(c), hysteresis loops are very square with a large remanence squareness, while they have a more complicated shape when the magnetic field is parallel to the steps (d). Clearly in this case, higher fields are required to drive the magnetization to saturation. According to the hysteresis loops in the two directions, we deduce that the EAM runs perpendicular to the steps. Whereas the shape anisotropy due to the steps always makes the EAM along the steps, the magnetocrystalline anisotropy at the step edges can establish an uniaxial magnetic anisotropy perpendicular or parallel to the steps. The competition between these two different anisotropies determines the EAM. In our system, the stronger step-induced anisotropy perpendicular to the steps dominates the in-plane anisotropy, leading to an EAM perpendicular to the steps. The remanence squareness in the longitudinal configuration, when the magnetic field is perpendicular to the steps, is shown in Fig. 3. The remanence squareness is always larger

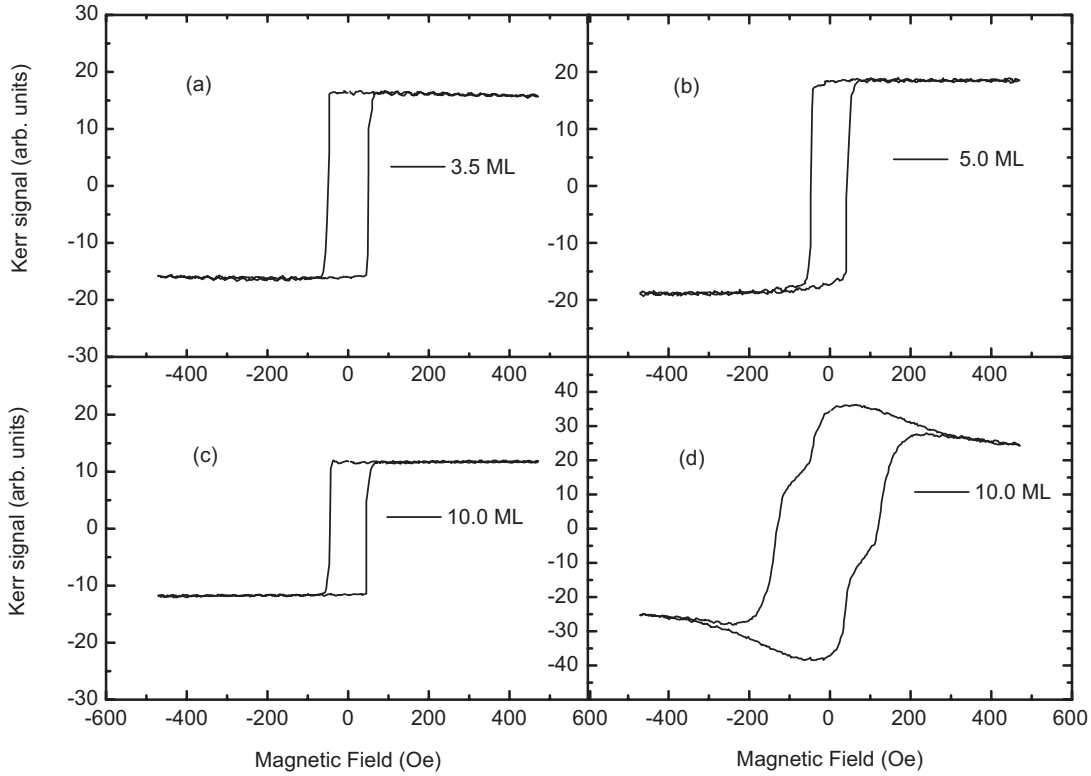

FIG. 4. Magnetic hysteresis loops of the Co films that are obtained in longitudinal configuration with the magnetic field [(a)–(c)] perpendicular and (d) parallel to the steps. The square loops correspond to the magnetic field perpendicular to the steps ($\perp$) for 3.5, 5.0, and 10.0 ML thick films. The sheared loop corresponds to the magnetic field parallel to the steps ($\parallel$) for a 10.0 ML thick film.

than 0.90 for films thicker than 3.5 ML, indicating that the EAM is hard to reorient by simply increasing the film coverage.

Similar results were reported for other systems, such as Fe/Ag(100),[29] Fe/W(001) (Refs. 30 and 31), and Co/Cu(100).[32–35] A step-induced uniaxial anisotropy was observed for ultrathin films grown on vicinal surfaces, which results in an in-plane orientation of the easy axis remaining parallel or perpendicular to the steps, depending on the thin film system, structure, and step density. This step-induced uniaxial anisotropy is believed to originate from two different contributions:[36] missing bonds at step edges and strain within the film induced by the step edge torque. Therefore, the effect of strain at step edges should also be considered in the step-induced magnetic anisotropy in addition to the effect of lattice symmetry breaking. In fact, Repetto *et al.*[28] reported that film-substrate interface effects play an important role for stepped surfaces. This contribution to the magnetic anisotropy can be much larger than the shape anisotropy, thus dominating the overall magnetic behavior and inducing an easy axis perpendicular to the steps rather than parallel to the steps.

B. Magnetic domain structure

The next point we address is the switching behavior from an out-of-plane to an in-plane magnetization during SRT. As is known for ultrathin systems, different types of SRT processes, such as canted magnetization or coexisting phases, can occur if higher order anisotropy[37] is considered. According to the higher order anisotropy contribution, there are different phases during SRT, which exhibit different micromagnetic structures.[38,39] So, we can investigate the detailed SRT process that can be either[40] a multidomain type, which includes the coexistence of perpendicularly and in-plane magnetized domains, or a spin canting type, which is accomplished by collective and continuous spin rotation. The question here is whether the out-of-plane remanence decreases due to splitting into domains or continuous rotation of the magnetization. We emphasize that one cannot discriminate between the two switching processes from hysteresis loops only because MOKE signal averages the contribution of the two facets. To resolve the magnetic microstructure of the Co films during the SRT, spatial X-PEEM microscopy in combination with XMCD has been performed. Figure 5 shows the X-PEEM images obtained for a 2.5 ML thick Co film: in the left panel (a), the beam incidence is parallel to the steps, while in the right panel (b), it is perpendicular to the steps. The different gray levels correspond to different projections of the local magnetization onto the direction of the incoming light.[41] Analysis of these levels for two X-PEEM images determines the local magnetization direction.[42] In Fig. 5(a), no clear magnetic contrast is observed, indicating that there is no component of the magnetization parallel to the steps. During our experiments, for the whole thickness region, we never observed obvious contrast to the x-ray incidence parallel to steps. In Fig. 5(b), however, two different periodic stripe contrasts are evidently visible in the image, indicating different projections of magnetization

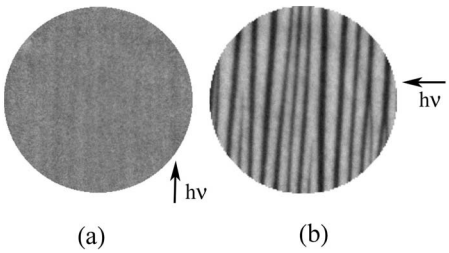

FIG. 5. Magnetic domain images of the as-grown 2.5 ML thick Co/Au(455) film. The field of view is 5 μm. (a) Magnetic domain patterns for an x-ray beam incidence parallel to the steps and (b) perpendicular to the steps, as indicated by the arrows labeled with $h\nu$.

perpendicular to the steps. Comparing images (a) and (b), we conclude that the magnetization distribution is confined to the plane determined by the [111] and [$\bar{2}$11] directions. The two stripes with different magnetic contrasts correspond to the two facets of Au(455) surfaces: in Fig. 5(b), the stripes with gray and black contrast levels correspond to the (677) and (233) facets, respectively. From a comparison of Figs. 5(a) and 5(b), we deduce that the local magnetizations have opposite projections along the beam and different canted magnetizations. Moreover, we clearly see that the SRT from out of plane to in plane has already started when the film coverage reaches 2.5 ML. From the different tilt angles off the normal direction for the two facets, we also deduce that the critical thickness for the transition is smaller for the (233) facets than for the (677) facets. This is consistent with the fact that for magnetization that is tilted out of plane, the tilt angle linearly depends on the vicinal angle when the magnetization has a component perpendicular to the steps. This is because the strength of the step-induced magnetic anisotropy increases with the vicinal angle.[43]

To investigate the SRT of the Co/Au(455) films in detail, a series of magnetic X-PEEM images have been recorded as a function of film thickness. Figure 6 shows the magnetic domain structure of the Co films when the x-ray beam incidence is perpendicular to the steps with different film thick-

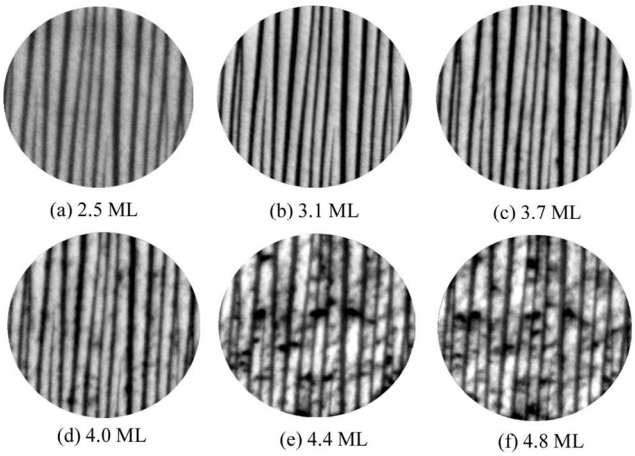

FIG. 6. Magnetic X-PEEM images for different thicknesses with an x-ray beam perpendicular to the steps.

nesses. For thicknesses ranging from 2.5 to 3.7 ML, regular magnetic stripes are observed. As the film coverage increases within this range, the magnetic contrast within each stripe (on the both facets) stays uniform and continuously becomes stronger, indicating that the magnetization rotates away from the out-of-plane direction. At the coverage of 3.7 ML, the magnetization lies almost in plane for the Au(233) facets. For the Au(677) facets, there is no apparent magnetic domain (within the 30 nm XMCD resolution), so we can infer that local magnetization is canted. This continuous SRT on the two facets is consistent with the square shape of the in-plane hysteresis loops that are obtained in the longitudinal MOKE configuration [Fig. 4(a)], which has a remanence squareness value of almost 1.0 (Fig. 3). In addition, the modulation period of the alternating magnetization direction is identical to the modulation period of the facets: the magnetic domain structure of the Co films replicates the surface structure of the substrate,[44,45] as predicted by calculations.[24] We then conclude that the magnetization crossover takes place by a continuous rotation from an out-of-plane to an in-plane preferred orientation for the (233) facet. When the film thickness further increases up to about 4.0 ML, two different processes occur for the two facets. For the (233) facet, the magnetic contrast level is completely black at 4.0 ML, and then the contrast decreases up to 4.8 ML due, as explained in the next paragraph, to the decrease in the uniaxial in-plane anisotropy relative to the shape anisotropy, which favors a parallel to the steps in-plane magnetization. For the (677) facet, the situation is clearly different: the magnetization changes from a uniform state to a multidomain state. Within the film thickness from 4.0 to 4.8 ML, small, in-plane magnetized, circular shape magnetic domains with the magnetization direction perpendicular to the steps appear at the facet edges. This observation is in agreement with the MOKE hysteresis loops (from 4.0 to 5.0 ML), for which the shape in longitudinal configuration is curved close to remanence [Fig. 4(b)], indicating a switching process by nucleation of small domains. Therefore, for the Au(677) facet, a continuous SRT occurs below 3.7 ML, and in-plane magnetization then splits into multidomains when the film is thicker than 4.0 ML.

Finally, the SRT that is observed in Co/Au(455) films can be summarized from the magnetic contrast of X-PEEM images, as shown in Fig. 6. The variation in the local XMCD asymmetry as a function of the film thickness can be reconstructed for the two facets (see Fig. 7). For the (233) facet, the SRT from out of plane to in plane mainly finished between 2.0 and 4.0 ML, in which the magnetic contrast continuously changes, keeping a uniform contrast level. The SRT in this facet can be attributed to a spin cantinglike transition, which is accomplished by collective and continuous rotation of the magnetization vector. When the film coverage is larger than 3.7 ML due to the vanishing effect of the in-plane anisotropy, the magnetic contrast begins to decrease. For the (677) facet, the SRT can be explained by two different processes. First, when the coverage is lower than 4.0 ML, the magnetic contrast is uniform and the magnetization direction continuously changes, corresponding to a continuous SRT as observed for the (233) facet. Second, when the coverage is higher than 4.0 ML, white and black domains appear with an in-plane magnetization perpendicular to the steps,

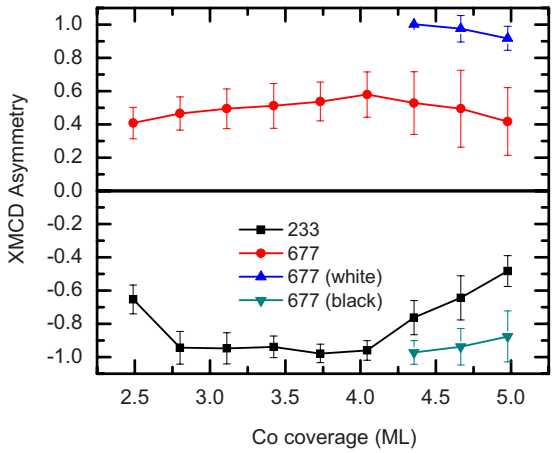

FIG. 7. (Color online) Normalized XMCD asymmetry of the Co films for the two facets as a function of the film thickness that is derived from the images in Fig. 6.

corresponding to a discontinuous SRT. The complicated SRT processes for Co/Au(455) films are associated with the competition of shape anisotropy (K_v), interface anisotropy (K_s), and step anisotropy (K_{step}) contributions to the effective anisotropy. If higher order anisotropy is considered, it was reported that interplay between first order anisotropy (K_1) and second order anisotropy (K_2) determines different magnetization switching behaviors, such as a continuous or discontinuous transition.[37,38] In our system, surface and step anisotropy can contribute to K_1, which can be written as $(K_1 = K_s/t + K_{\text{step}}/tw + K_v$, where t is the film thickness and w is the step width). For the Au(233) facet, due to the dominant role of K_{step}, it is possible to stabilize a canted magnetization during SRT. Since K_{step} anisotropy effect decreases with increasing film coverage, the step anisotropy (perpendicular to the steps) becomes comparable to the shape anisotropy (parallel to the steps), resulting in the decreasing contrast in Au(233) facet above 4.0 ML. For Au(677) facet, we find coexisting phases. The two different SRT processes on the two facets can be associated with different relations between K_1 and K_2, which may come from several possibilities. First, the Co ultrathin film crystalline structure is not exactly same on the two facets,[6,7] which exhibits different anisotropies. Second, these two facets are vicinal surface with different step densities, which can induce different step anisotropies on each facet. If we consider these different contributions to the effective magnetic anisotropy, it is not surprising to have different relations between K_1 and K_2, which can result in different SRTs on the two facets. The quantitative analysis of the origin of higher anisotropy is beyond the scope of this paper for this complicated system.

IV. SUMMARY

In summary, Co ultrathin films have been grown on faceted Au(455) surfaces, and the SRT has been investigated by MOKE measurements and X-PEEM experiments. From the X-PEEM images, we observe magnetic stripped domains that replicate the underlying periodic faceted substrate. With

increasing film thickness, different SRT processes occur for the two facets. The SRT proceeds via a state of uniform magnetization canting for the (233) facet within the thickness region between 2.0 and 4.0 ML, whereas the transition involves the continuous transition below 3.7 ML that is followed by the formation of small in-plane multidomains at film thickness larger than 4.0 ML for the (677) facet. Furthermore, the preferred direction of magnetization reorients itself from out of plane to in plane perpendicular to the atomic steps due to the dominant contribution of the step-induced magnetic anisotropy.

ACKNOWLEDGMENTS

The authors would like to thank the technical staff at Elettra for their assistance during the XMCD-PEEEM experiments and Y. Nahas for her help during MOKE experiments. We wish to thank W. Kuch and Y. Z. Zheng for many interesting discussions on the experiment analysis, especially in the early stage of the work. We also thank S. Mehendale for her critical reading. This work was supported by the French "Ministère de l'Éducation National et de l'Enseignement Supérieur."

*Corresponding author: yann.girard@univ-paris-diderot.fr

[1] *Ultrathin Magnetic Structures*, edited by B. Heinrich and J. A. C. Bland (Springer-Verlag, Berlin, 2004).
[2] J. Shen, Z. Gai, and J. Kirschner, Surf. Sci. Rep. **52**, 163 (2004).
[3] T. C. Ulbrich, D. Makarov, G. Hu, I. L. Guhr, D. Suess, T. Schrefl, and M. Albrecht, Phys. Rev. Lett. **96**, 077202 (2006).
[4] N. Weiss, T. Cren, M. Epple, S. Rusponi, G. Baudot, S. Rohart, A. Tejeda, V. Repain, S. Rousset, P. Ohresser, F. Scheurer, P. Bencok, and H. Brune, Phys. Rev. Lett. **95**, 157204 (2005).
[5] S. Rohart, V. Repain, A. Tejeda, P. Ohresser, F. Scheurer, P. Bencok, J. Ferré, and S. Rousset, Phys. Rev. B **73**, 165412 (2006).
[6] Y. Girard, G. Baudot, V. Repain, S. Rohart, S. Rousset, A. Coati, and Y. Garreau, Phys. Rev. B **72**, 155434 (2005).
[7] G. Baudot, Y. Girard, V. Repain, S. Rohart, S. Rousset, S. Kreckelbergh, A. Coati, and Y. Garreau, Surf. Sci. **557**, 171 (2004).
[8] *Magnetic Microscopy of Nanostructures*, edited by H. Hopster and H. P. Oepen (Springer, Berlin, 2005).
[9] P. J. Jensen and K. H. Bennemann, Surf. Sci. Rep. **61**, 129 (2006).
[10] J. Shen and J. Kirschner, Surf. Sci. **500**, 300 (2002).
[11] K. Amemiya, E. Sakai, D. Matsumura, H. Abe, T. Ohta, and T. Yokoyama, Phys. Rev. B **71**, 214420 (2005).
[12] T. Nakagawa, H. Watanabe, and T. Yokoyama, Phys. Rev. B **71**, 235403 (2005).
[13] A. Enders, D. Peterka, D. Repetto, N. Lin, A. Dmitriev, and K. Kern, Phys. Rev. Lett. **90**, 217203 (2003).
[14] D. Peterka, A. Enders, G. Haas, and K. Kern, Phys. Rev. B **66**, 104411 (2002).
[15] R. Allenspach and A. Bischof, Phys. Rev. Lett. **69**, 3385 (1992).
[16] A. Vaterlaus, C. Stamm, U. Maier, M. G. Pini, P. Politi, and D. Pescia, Phys. Rev. Lett. **84**, 2247 (2000).
[17] Y. Z. Wu, C. Won, A. Scholl, A. Doran, H. W. Zhao, X. F. Jin, and Z. Q. Qiu, Phys. Rev. Lett. **93**, 117205 (2004).
[18] H. W. Zhao, C. Won, Y. Z. Wu, A. Scholl, A. Doran, and Z. Q. Qiu, Phys. Rev. B **70**, 024423 (2004).
[19] C. Won, Y. Z. Wu, J. Choi, W. Kim, A. Scholl, A. Doran, T. Owens, J. Wu, X. F. Jin, and Z. Q. Qiu, Phys. Rev. B **71**, 224429 (2005).
[20] J. Choi, J. Wu, C. Won, Y. Z. Wu, A. Scholl, A. Doran, T. Owens, and Z. Q. Qiu, Phys. Rev. Lett. **98**, 207205 (2007).
[21] R. Allenspach, M. Stampanoni, and A. Bischof, Phys. Rev. Lett. **65**, 3344 (1990).
[22] J. Pommier, P. Meyer, G. Pénissard, J. Ferré, P. Bruno, and D. Renard, Phys. Rev. Lett. **65**, 2054 (1990).
[23] M. Speckmann, H. P. Oepen, and H. Ibach, Phys. Rev. Lett. **75**, 2035 (1995).
[24] A. Tejeda, G. Baudot, V. Repain, S. Rousset, J. Ferré, J. P. Jamet, A. Thiaville, and L. Barbier, Europhys. Lett. **71**, 117 (2005).
[25] S. Rousset, F. Pourmir, J. M. Berroir, J. Klein, J. Lecoeur, P. Hecquet, and B. Salanon, Surf. Sci. **422**, 33 (1999).
[26] S. Rousset, J. M. Berroir, V. Repain, Y. Garreau, V. H. Etgens, J. Lecoeur, and R. Pinchaux, Surf. Sci. **443**, 265 (1999).
[27] S. Rousset, V. Repain, G. Baudot, H. Ellmer, Y. Garreau, V. Etgens, J. M. Berroir, B. Croset, M. Sotto, P. Zeppenfeld, J. Ferré, J. P. Jamet, C. Chappert, and J. Lecoeur, Mater. Sci. Eng., B **96**, 169 (2002).
[28] D. Repetto, T. Y. Lee, S. Rusponi, J. Honolka, K. Kuhnke, V. Sessi, U. Starke, H. Brune, P. Gambardella, C. Carbone, A. Enders, and K. Kern, Phys. Rev. B **74**, 054408 (2006).
[29] R. K. Kawakami, E. J. Escorcia-Aparicio, and Z. Q. Qiu, Phys. Rev. Lett. **77**, 2570 (1996).
[30] H. J. Choi, Z. Q. Qiu, J. Pearson, J. S. Jiang, Dongqi Li, and S. D. Bader, Phys. Rev. B **57**, R12713 (1998).
[31] J. Chen and J. L. Erskine, Phys. Rev. Lett. **68**, 1212 (1992).
[32] R. K. Kawakami, M. O. Bowen, H. J. Choi, E. J. Escorcia-Aparicio, and Z. Q. Qiu, Phys. Rev. B **58**, R5924 (1998).
[33] T. Nakagawa, H. Watanabe, and T. Yokoyama, Phys. Rev. B **74**, 134422 (2006).
[34] A. Berger, U. Linke, and H. P. Oepen, Phys. Rev. Lett. **68**, 839 (1992).
[35] W. Weber, C. H. Back, A. Bischof, Ch. Würsch, and R. Allenspach, Phys. Rev. Lett. **76**, 1940 (1996).
[36] D. S. Chuang, C. A. Ballentine, and R. C. O. Handley, Phys. Rev. B **49**, 15084 (1994).
[37] H. Fritzsche, J. Kohlhepp, H. J. Elmers, and U. Gradmann, Phys. Rev. B **49**, 15665 (1994).
[38] *Competing Interactions and Pattern Formation in Nanoworld*, edited by Elena Y. Vedmedenko (Wiley, New York, 2007).
[39] Y. Millev and J. Kirschner, Phys. Rev. B **54**, 4137 (1996).
[40] M. A. Torija, J. P. Pierce, and J. Shen, Phys. Rev. B **63**, 092404 (2001).
[41] W. Kuch, *Magnetism: A Synchrotron Radiation Approach*, Lecture Notes in Physics Vol. 697 (Springer, Berlin/Heidelberg, 2006), pp. 275–320.

[42] W. Kuch, X. Gao, and J. Kirschner, Phys. Rev. B **65**, 064406 (2002).
[43] Y. Z. Wu, C. Won, H. W. Zhao, and Z. Q. Qiu, Phys. Rev. B **67**, 094409 (2003).
[44] S. P. Li, W. S. Lew, J. A. C. Bland, L. Lopez-Diaz, M. Natali, C. A. F. Vaz, and Y. Chen, Nature (London) **415**, 600 (2002).
[45] S. P. Li, W. S. Lew, J. A. C. Bland, L. Lopez-Diaz, C. A. F. Vaz, M. Natali, and Y. Chen, Phys. Rev. Lett. **88**, 087202 (2002).